

Flow measurements over a moving sandy bed

by

Costa, MAV; Teixeira, SFCF and Teixeira, JCF

School of Engineering

University of Minho

4800-058 Guimarães, Portugal

ABSTRACT

In understanding the behaviour of estuary sediment beds, the phenomenon associated with the motion of suspended particles entrained from the surface is of great relevance. Experiments investigating the flow dynamics in the vicinity of the surface were carried out on a mini circular flume, 131 mm in diameter. The velocity field was measured at two Reynolds number using a two colour, two component LDA system. The simulated bed consisted of a glycerine solution and a range of polymeric and glass beads with various sizes (250 – 2,850 μm) and densities (1,050 – 2,600 kg/m^3). Measurements were made upon deformable and rigid smooth and rough beds.

Generally, results show the existence of three moving dunes inside the perimeter of the flume, whose characteristics depends on the type of beads applied. It is observed that the flow patterns are time dependent and related the rate of sediment transport by the moving fluid. The effect of the particle size upon the fluid turbulence was also investigated and it was verified that smaller particles form a more deformable bed than larger particles, interfering with the shear stress. It was also observed that particle concentration is an important factor in controlling flow turbulence. On the other hand, turbulence is enhanced upstream of the dune, what may be related with the reduction of the boundary layer thickness. The results have shown that the phenomena associated with surface deformation, proved to be the main flow characteristic that influences the velocity profile, turbulence energy production and shear stresses.

The figure below shows a frame from a video movie depicting the behaviour of a deforming bed.



1. INTRODUCTION

The contribution of entrained particles in suspension and transported by the flow to the turbulence is one of the most important fact having into account during the erosion process investigation.

For flows that exceed the threshold of motion, an initially flat bed may deform into various types of bed feature, ranging in size from small ripples up to large dunes (Soulsby, 1997). The height and wavelength of these dunes are governed by the water depth as well as the bed shear stress. In the same way, Prent and Hickin (2001) refer that the water depth is the limiting factor of dune growth and is therefore best used to examine the response of dunes to their flow environment. According regression models got by these authors, the dune length is approximately 12 or 17 times the dune height. Some investigators suggest that the loss of dune mass to suspended load can flatten the shape of a dune as flow magnitude increases. Furthermore, the shear exerted on a dune reaches a maximum at the dune crest (Prent and Hickin, 2001).

Bed load transport is controlled by the velocity field of the fluid, and thus by the mean shear stress and the size and arrangement of the particles on the bed. Hetsroni (1989) stated that for a given particle size, the turbulence intensity at the centreline was reduced, however, close to the wall it increased for certain values of particle concentration.

For speeds significantly above the threshold of motion, particles are entrained off the bed and into suspension, where they are carried at the same velocity as the fluid. When it happens, the proportion of particles transported in suspension is generally much larger than that being carried simultaneously as bed load, and consequently the suspended load is an important contribution to the total sediment transport rate. The grains remain in suspension if their settling velocity is smaller than the upward turbulent component of the velocity. Besides, the bedform height determines from which depth below the initial bed level the bed sediment is entrained (Kleinhans, 2001).

The present work aims to understand the behaviour of estuary sediment beds and for that, some experimental work was carried out to study the phenomenon associated with the motion of suspended particles entrained from the bed surface.

2. EXPERIMENTAL DETAILS

Experiments were performed using a toroidal mini flume, whose design has been extensively used in critical shear stress measurements in sediment beds (Graham et al, 1992), allowing the reproduction of the main flow characteristics near the sediment, as observed in natural beds. It consists of two concentric tubes, 70 mm high, the internal diameter of the outer tube is 131 mm and the outer diameter of the inner wall is 60 mm. The walls are 3 and 2.5 mm thick for the outer and inner, respectively. The inner tube is made of Perspex, while the outer is built in quartz for better optical access. The entire flume is enclosed in a square box to minimise the optical distortions resulting from the combination of a mismatch in the refractive index and a circular surface. The space between the box and the flume was also filled with water. A circular lid linked to the shaft of a Physica MC1 rehometer on top of the toroidal channel drives the fluid on a tangential flow at controllable speeds.

A schematic arrangement is shown in Figure 1.

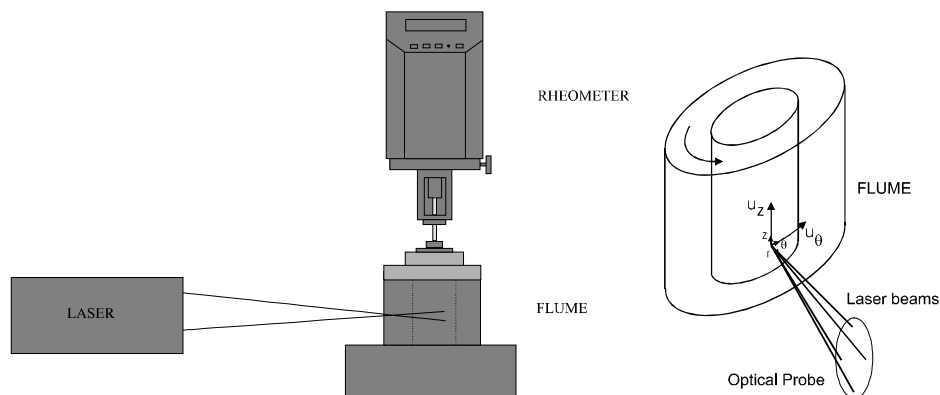


Figure 1- Schematic view of the test section.

A two colour/four beam – two component LDA system was used to measure simultaneously the tangential and axial components of the velocity.. In this, a water cooled, 5 W, Argon-Ion laser beam is splitted into two colours (514.5 and 488 nm) and the resulting beams are steered into the transmitting optics through a fibber optic cable, 5 m long. The transmitting lenses are standard Dantec, 310 mm in focal length resulting in a half angle between the beams of 6.90 and 7.17°, respectively. Flow direction sensitivity is provided through 40 MHz Bragg cells on both components. The scattered light is collected in the backscatter mode through the same 310 mm lens and steered through the fibber optical cable into two photomultipliers. The transmitting/receiving optics are mounted in a 3D programmable traversing table and the Doppler signals were processed through a couple of spectrum analysers (Dantec BSA’s 55x models). The beams have an expansion factor of 1.95 and the resulting probe volume is around 0.08 mm in diameter and 0.6 mm long.

An update to the transmitting optics, in which the transmitting beams are tilted by as much as the half angle, was made in order to enable the velocity measurements in the close vicinity of the bed.

Polyamide particles (20 μm and density of 1030 kg/m3) were used as seeding medium, once they do not interfere with the flow properties.

All the hardware control, set up, configuration, data acquisition and processing is controlled by an integrated software package, Dantec BSAFlow V 1.41.

Figure 2 shows a schematic view of the optical experimental arrangement.

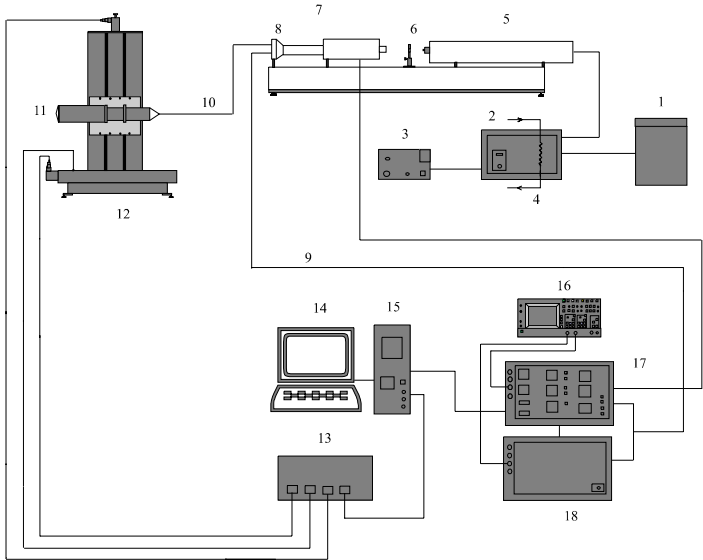


Figure 2- Schematic layout of the LDA instrumentation.

- | | | |
|-----------------|----------------------------------|-----------------------------|
| 1- Transformer | 7- Beam separator and Bragg cell | 13- Traverse controller |
| 2- Power supply | 8- Fibber manipulators | 14- Monitor |
| 3- Controller | 9- Scattered signal | 15- Computer |
| 4- Water flow | 10- Fibber optic | 16- Oscilloscope |
| 5- Laser head | 11- Transmitting optics | 17- Burst Spectrum Analyser |
| 6- Shutter | 12- 3D Traverse table | 18- Burst Spectrum Analyser |

3. TEST CONDITIONS

In order to accurately study the erosion mechanism and because of its complexity due to the simultaneous contribution of various factors, it is of crucial importance the evaluation at controlled conditions.

Firstly, experiments took place on both a smooth (SB) and a rough (RB1) surface (lower wall of the flume). The rough bed was moulded in gypsum over a natural sediment, in order to reproduce the roughness and shape of the sediment bed, and presents a mean roughness height of 0.571 mm (Costa *et al*, 2001).

Based on the rheological properties of the sediment laden fluid (obtained from erosion tests in natural muds) and once it is fundamental to apply a suitable fluid from the physical properties point of view and that of optical compatibility, an aqueous solution of glycerine (concentration = 366.2 kg/m³; density = 1076.2 kg/m³ and viscosity= 0.003 N/sm) was used as a test fluid.

For a better understanding of the physical mechanisms leading to bed erosion, the investigation of the influence of suspended particles upon the flow configuration is of great importance. This may be of greater relevance not only on the initial stages but in the stages when matter has already been entrained into the carrier fluid. Depending on particle size and concentration, the flow field may be modified by the energy exchanges between the continuous and dispersed phases resulting from particle transport.

In order to make a comprehensive evaluation of such contributions, a wide set of beads was tested. The size choice was based on various factors: commercial availability; relevance to the natural conditions (that is, how close to the size range measured in natural sediments); feasibility. Thus, very small particles are most likely to follow fluid turbulence and their contribution will be difficult to assess. Furthermore, they will be easily entrained into the fluid and a homogeneous solution will be formed; light penetration will be reduced and measurements made difficult. Most of the particles are made of glass, although for lower sizes, polymeric beads are those available.

Combining these factors, tests were done using different ranges of size and densities of particles, as summarised in Table 1.

Table 1- Ranges of particle size and density.

Particles	Range (μm)	Density (kg/m^3)
Polymer micro spheres (P1)	250 - 750	1,050
Glass beads (P2)	850 – 1,400	2,600
Glass beads (P3)	1,400 – 1,700	2,600
Glass beads (P4)	1,700 – 2,850	2,500

Due to the density difference between the liquid and the particles, when the liquid is stationary, a layer of particles is formed at the bottom. When the fluid is set in motion, the flow drag deforms the bed and moving “dunes” are formed on the bed. This configuration yields both a moving (deformable) bed and a suspension because bed deformation occurs by the movement of the top layer of particles, entrained into the moving liquid and deposited further downstream. This whole process is depicted in Figure 3. Because LDA is a point measurement technique, on this particular flow configuration, velocity statistics have to be related to the relative position to the moving bed. Thus, measurements were carried out, at each point, over a period of time long enough to span at least the entire rotation period of the deforming bed. At each point above the surface, the experiments were initiated at the same relative position to the bed in order to synchronize all the measurements with the deforming bed.

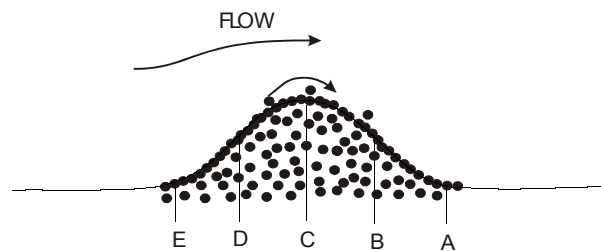


Figure 3- Most relevant positions of the dune during measurements.

In order to keep the particle/fluid density ratio approximately constant, the experiments with the smaller particles (P1) were carried out using ethyl alcohol as fluid as opposed to aqueous solution of glycerine. Therefore, in order to have similar Reynolds numbers, these experiments were carried out at lower velocities. Investigations were taken at Reynolds numbers of 27,000 and 54,000. Data were always obtained at approximately 8 mm from the outer wall (where the phenomena associated with the sediment erosion is more relevant) and from the basis of the dune up to around 10 mm above the crest.

4. RESULTS AND DISCUSSION

During the experiments, it was possible to observe the formation of three similar dunes simultaneously, equally spaced along the perimeter, which are continuously deformed by the moving fluid (Figure 3). The formation of these dunes may be related with the existence of secondary flows typical from the flume.

Although, the quantity of the various beads inside the flume was similar (approximately 326 kg/m^3), the height of the dunes was different: 15, 11 and 8 mm for different size beads P1, P2 and P3, respectively. Concerning the particles P4, it was not possible to observe any dune once the beads were evenly dispersed in the flume at higher Reynolds number and practically did not move at lower velocities. These differences are related with the settling velocity of the particles, which is very small to the beads P1 and too high to particles P4, when compared with the mean velocity of the flow. Due to the difference in height of the dunes and because the distance from the basis of the dune to the measuring point is changing with time, the curves of the graphs presented will have different time lengths.

For each measuring point, the data consisted of a time series long enough to accommodate the entire rotation of the bed. This time length varies with the particle size and the lid rotation speed. Figure 4 shows a typical time series for the instantaneous velocity (beads P3, at $\text{Re} = 54\,000$ and at 18 mm distance from the basis of the dune). From these data it is observed that the mean velocity has a periodic behaviour due to the particle movement; therefore, the mean velocity has to be calculated along the time as a moving average, which is also shown in Figure 4. Furthermore, the higher order moments (*rms*) can also be retrieved from this data, as a function of time. It should be emphasized that, in knowing the perimeter of the flume, a time scale can be converted into a position scale.

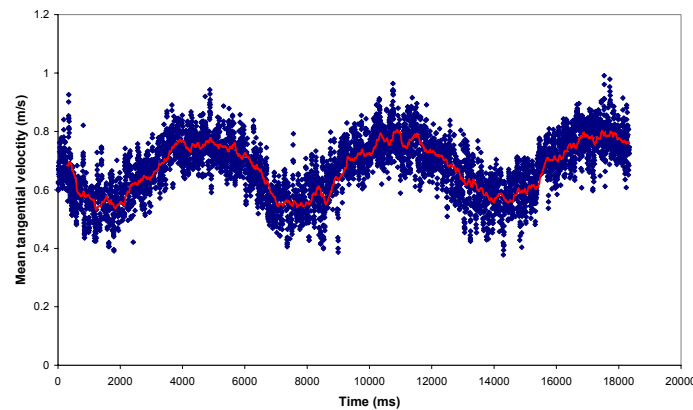


Figure 4- Mean tangential velocity; beads P3; $\text{Re} = 54,000$; $y = 18 \text{ mm}$.

Extending this procedure for all the measuring points across a vertical direction, velocity profiles along the moving bed can be obtained. Figure 5 presents the mean tangential velocity profiles for beads P3, at $\text{Re} = 54,000$, at selected positions from the basis of the dune (distances of 1, 3, 7, 9 and 16 mm).

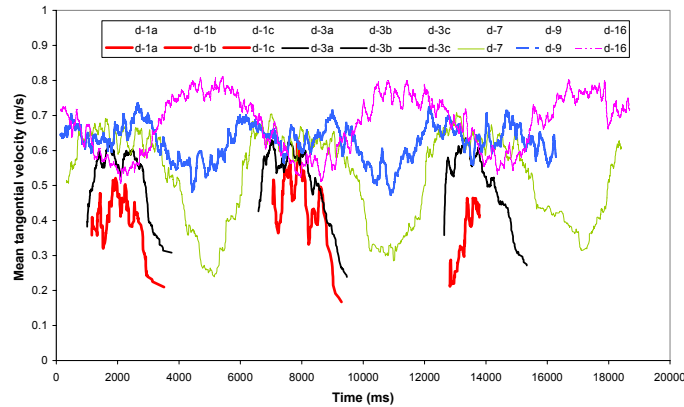


Figure 5- Mean tangential velocity profiles at different distances from the surface.

This Figure was obtained by plotting the moving average of the tangential velocity, for each position. In order to visually simplify the graph, just a few selected positions are presented, along the vertical axis from the dune. From Figure 5, it is possible to observe the effect of the moving bed.

The broken lines concerning a few positions closer to the surface are due to the absence of any data, as the moving bed periodically submerges the probe volume.

From the figure, it can be observed that a peak of the first dune occurs at $\cong 5s$. Due to the close proximity of the measuring point to the surface, velocity here is lower than at regions in between two consecutive dunes (at $\cong 2s$). As the measuring point is moved upwards the effect of the boundary layer near the lower wall is reduced and the velocity is primarily controlled by the available cross section area (local gap between the “sediment” and the upper driving lid), which is reduced on top of a crest. Therefore, the average velocity is higher at that location than in other regions.

Taking the data from all the measuring points at a certain position in time allows the construction of vertical profiles. Of all the possible positions, 5 of them were systematically taken, as represented in Figure 3, they are referred to positions A, B, C, D and E. Positions A and E are physically equivalent.

Figure 6 presents the mean tangential velocity, at positions A, B, C, D and E, for beads P3, at $Re = 54,000$. The distance to wall refers to the distance (y) from the local dune surface. Similar profiles are also observed for other flow Reynolds numbers.

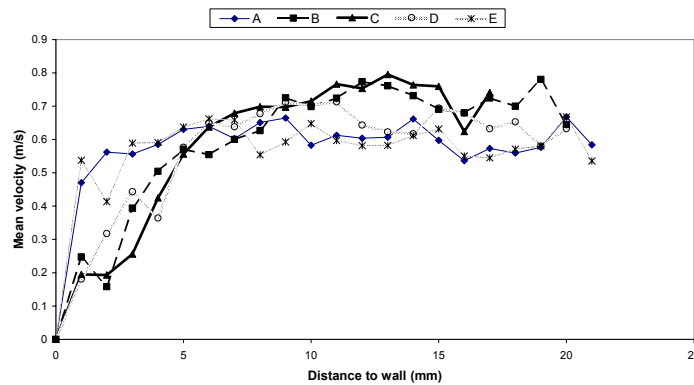


Figure 6- Mean tangential velocity at various positions along the dune.

Local averages are based on samples of limited size centred on the various positions previously referred (A, B, C, D, E). Therefore, certain statistical uncertainty is linked to the data, particularly for the higher order velocity moments. However, it can be observed that, as expected, positions A and E are similar indeed (Figure 6).

From the previous data, several fundamental features must be referred. Firstly, no flow separation is observed downstream of the moving dunes (positions A and B). This may be due to the fact that the dune amplitude to

wavelength ratio is small which reduces the possibility of flow separation downstream. Another contributing factor is likely to be the bed deformation, which reduces the risk of flow separation. Further evidence on this will be shown subsequently. Secondly, the crest of the dunes is the region that shows the lower velocity gradients, although the cross section area is smaller. This observation is in agreement with the hypothesis previously put forward of bed deformation reducing the local stresses and gradients. This fact yields an interesting characteristic to the flow. Figure 6 shows that the mean flow velocity is higher above the throat of the dunes than above its crest. Because the velocity at the top of the flume is the same (boundary condition), due to mass conservation, the flow velocity in the regions closer to the rotating lid must be inverse to those near the sediment: the flow velocity is higher above the crest and lower above the throat. As a consequence, a periodic instability occurs along the flume in which the flow is driven upwards upstream of the dune and downwards downstream the crest of the dune. This mechanism is the main factor for particle entrainment and deposition, along the model sketched in Figure 3.

Figure 7 shows the profile for the total shear stress, including both the laminar ($\mu \partial U / \partial y$), which is dominant near the interface, and the turbulent ($-\rho \langle uv \rangle$) components.

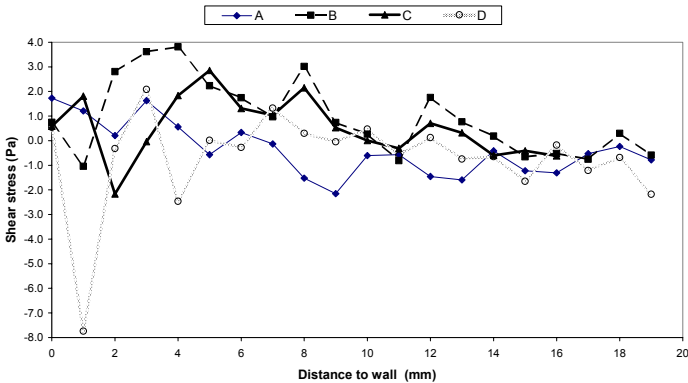


Figure 7- Shear stress at various positions along the dune.

In this Figure, positions B and D are quite dissimilar. In fact, they refer to different positions on the flow: B is downstream of the dune and D is a position upstream of that. Due to the flow development, the boundary layer for position B is larger than that of D (Figure 6) and, therefore, the velocity profile shows a region close to the surface, of lower gradients (thus lower shear stresses). The higher shear stresses in position D are responsible for the particle drag and subsequent entrainment into the main flow, which is the driving mechanism for the bed deformation and motion.

The shear stress for the deformable bed is compared with other surfaces: smooth (SB) and a rigid rough bed (RB1), as shown in Figure 8.

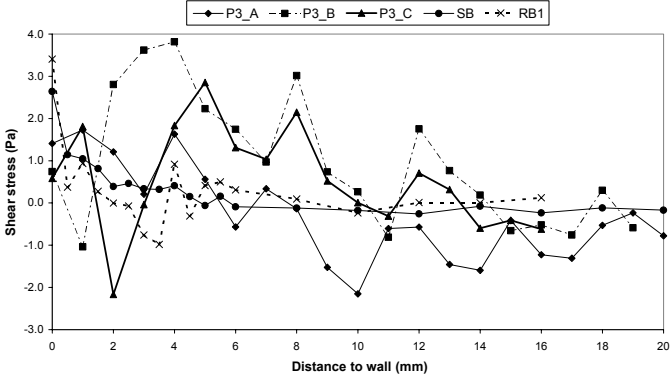


Figure 8- Shear stress on a moving, a smooth and a rough bed.

It is observed that the surface shear stress is lower for a deforming bed than for a rigid surface. Similar observations have been reported in other flow configurations. In addition, shear stress near the crest (position C) is lower than near the throat. It must be pointed out that the surface deformation is stronger near the crest than in other regions along the dune surface (lowering the local shear stress), which is in agreement with the flow patterns above described.

Figures 9 and 10 show the effect of particle size upon fluid turbulence for different Reynolds numbers. Results can be compared with those obtained from a smooth bed, as a reference. In these processes, the second order moments were calculated on average for the entire time series. This is a reasonable approach because (Figure 4) the data spread remains fairly constant throughout the duration of the experiments. The data show that turbulence near the surface is similar, although higher to that observed on a solid surface. However, for regions further apart from the surface, the fluid turbulence remains at a much higher level. This may be due to the fact that the bed deformation is made up of a succession of particles entrained into the main flow, transport over the dune, and subsequent deposition. This whole process enables the transportation of energy into regions further away from the surface, increasing the flow turbulence.

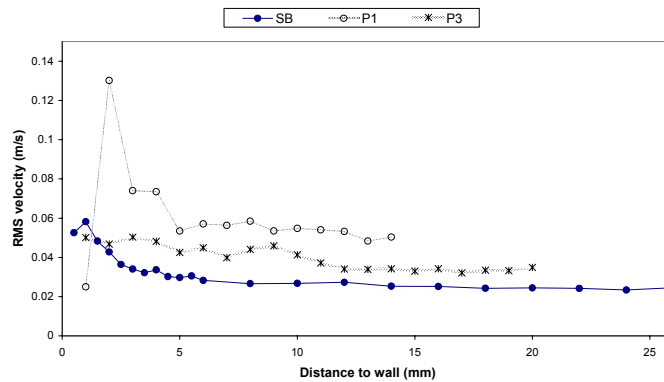


Figure 9- Turbulence profile; beads P1 and P3; Re = 27,000.

The data also show the effect of particle concentration (that is bigger to the smaller particles as a result of lower density ratio). Although the actual fluid velocity is lower (same Re for different fluids), the particles P1 show higher turbulence than larger particles, as discussed by Azzopardi and Teixeira (1994).

Figure 10 shows the influence of particle size (see Table 1), for an approximately particle concentration. Due to velocity slip between the phases, the fluid turbulence increases in the presence of larger particles.

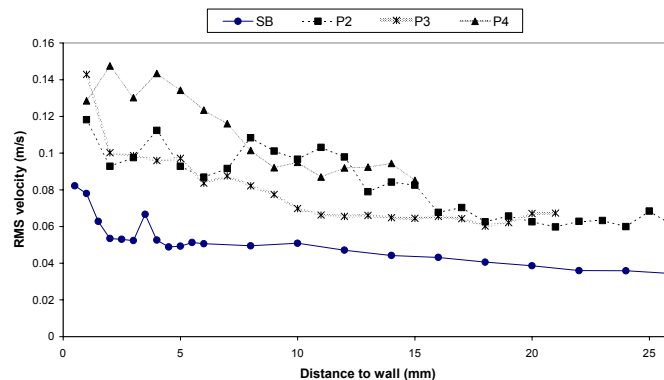


Figure 10- Turbulence profile; beads P2, P3 and P4; Re = 54,000.

The effect of fluid Reynolds number is shown in Figure 11. It can be observed that increasing the fluid velocity, the enhancement of turbulence is stronger near the surface. By increasing the velocity, boundary layer thickness reduces and so does the laminar sub layer. Thus, roughness effects are expected to be stronger near the surface at such high Reynolds numbers.

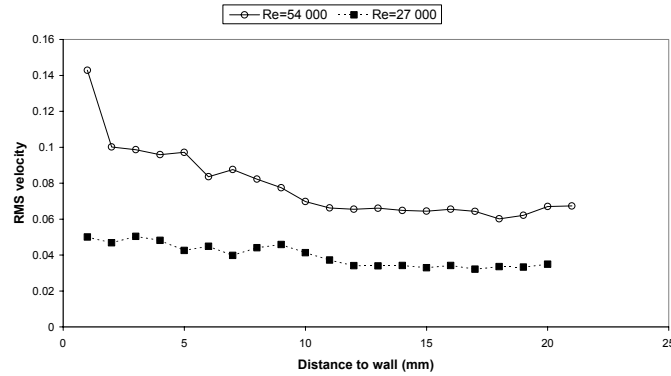


Figure 11- Turbulence profile; beads P3; Re = 54,000 and Re = 27,000.

The effects of the surface roughness upon the turbulence patterns are presented. Smooth and the rough beds with the bed made up of beads P4 are compared at Re = 27,000. The large size of the particles allows a nearly absence of large scale motion (at these conditions, the beads closely approach a rigid rough wall).

The free stream velocity (U_e), the boundary layer thickness (δ) (which correspond to the velocity of 99.5 % of U_e) and the shear velocity ($u_{\tau} = (\tau_w/\rho)^{0.5}$) for the three beds are presented in Table 2.

Table 2- Boundary layer characteristics of the test beds.

	δ (mm)	u_{τ} (m/s)	U_e (m/s)
SB	9.95	0.0317	0.3705
RB1	2.49	0.0324	0.4440
P4	7.96	0.01498	0.4142

Figure 12 presents the mean velocity profiles for the beds SB, RB1 and using P4 as a function of the distance from the bottom wall (y). The symbol “+” denotes normalization by the shear velocity.

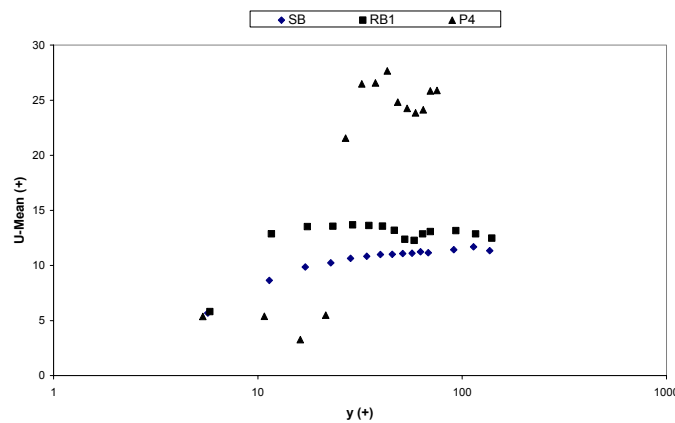


Figure 12- Mean velocity profile.

Figure 12 shows the shift in the velocity profile from smooth wall to the rough surface and from this to a sandy bed. Although both RB1 and P4 beads have roughness, this observation suggests that their behaviour is very dissimilar. The results concerning surface beads P4 may be affected by the small scale motion of particles dragged by the flow. This local motion at the surface reduces the fluid velocity gradient, which may show oscillation in the vicinity of the surface, reducing the local shear stress. From these data, the parameters of the log law for the velocity profile can be calculated and were shown to be much smaller than those defined by the

von Karman constant ($k = 0.41$). This may be due the occurrence of secondary flows and a complex pattern of recirculation zones in the vicinity of the wall. Further insight can be gained from Figure 13, which shows the normalized velocity defect across the boundary layer.

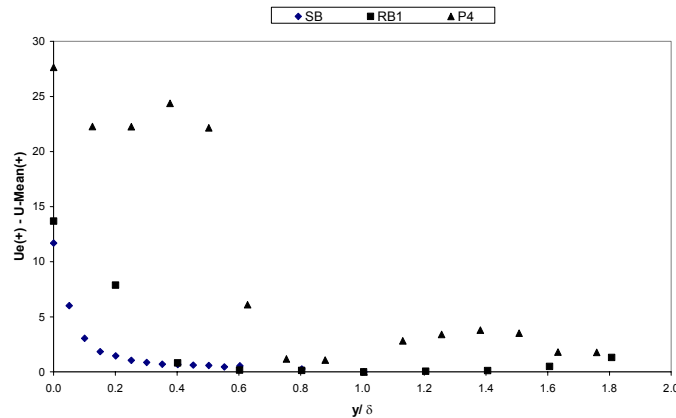


Figure 13- Mean velocity defect.

The deviation in the velocity defect near the surface from that observed over a rigid bed suggests that although the momentum transport in the fluid is not entirely wall driven and the singular characteristics of the toroidal flow in the flume (secondary flow, recirculation bubbles), may play an important role in momentum transfer in the boundary layer. Furthermore, the local deformation of the ‘sandy’ bed is a crucial mechanism.

Figure 14 presents the Reynolds normal stresses in the streamwise x direction. u is the fluctuating velocity components and the angular brackets denotes time averaging. This normal stress shows considerable sensitivity to the boundary conditions in the vicinity of the surface. Such behaviour was also observed by Krogstad and Antonia (1999) in different flow configurations.

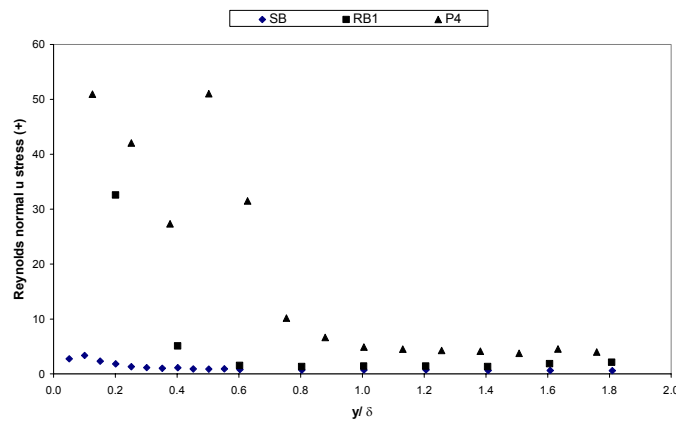


Figure 14- Reynolds normal stresses, $\langle u'^2 \rangle$.

The Reynolds shear stresses are shown in Figure 15.

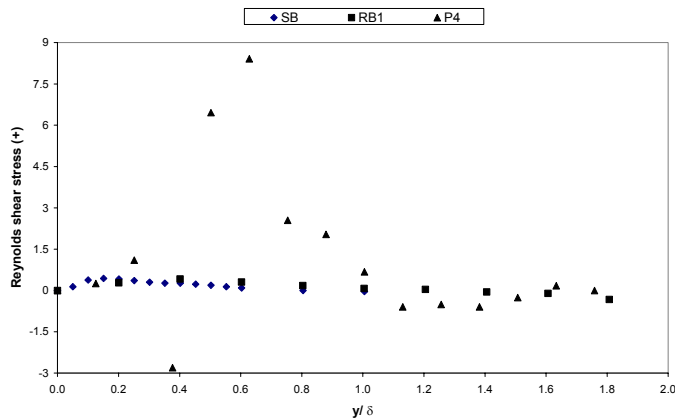


Figure 15- Reynolds shear stresses, $\langle -u^+v^+ \rangle$.

From this Figure, it may be concluded that the turbulent shear stresses are of prime importance in the regions closer to the wall although they approach zero in the laminar sub layer. In addition, on a flow over a non rigid sandy bed, the maximum of the shear stress is shifted into a region further away from the wall, when compared with the flow over either a smooth or a rough surface. This may be due to the enhanced turbulent momentum transfer in the crosswise direction occurring due to particle entrainment to the flow.

The profile for the turbulent energy production is shown in Figure 16, for all the surfaces compared in this study. On a flow over a rough sandy surface, mainly with the beads, the maximum of the shear stress is shifted into a region further away from the wall, when compared with the flow over a smooth surface. Furthermore, the rate of turbulence production shows considerable higher value than that observed over a rigid surface. This may be due to the enhanced turbulent momentum transfer in the crosswise direction occurring due to particle entrainment.

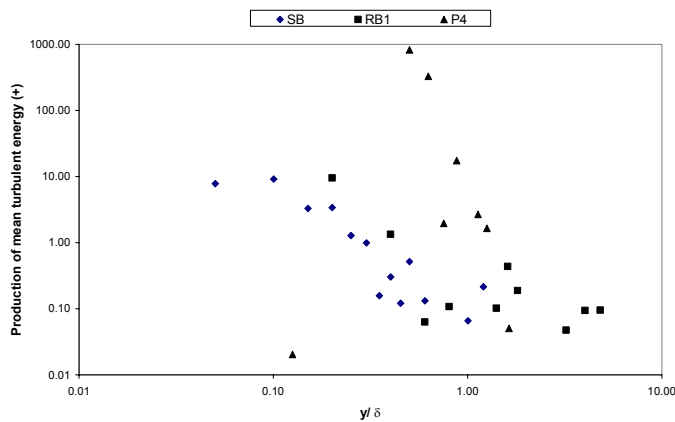


Figure 16- Rate of production of mean turbulent energy.

5. CONCLUSIONS

The use of glass/polymer beads is an effective way of simulating a moving bed. Some of the features observed in an eroding sediment are duplicated in this artificial system: entrainment of particles into the main flow, transport and subsequent deposition. Furthermore, as the resulting bed moves, it is similar a deforming sediment in which the shear stress at the interface is lower than that on a rigid surface. The flow patterns along the moving surface have been identified and described based upon the information retrieved from the velocity time series data. From this, it has been found that the upstream face of the bed roughness is that more prone to erosion, due to the higher shear stress in this region. Downstream, the opposite is observed: lower velocity gradients in which the shear stress approaches zero.

The particle size, which increases local roughness, enhances turbulence near the interface. In addition, higher turbulence levels are observed further way from the wall (when compared with a solid rough surface) due to momentum transport by the entrained particles. If the conditions are appropriate (that is lower density ratio and smaller particles) a very high concentration of particles can be observed. It was also found that turbulence increases with particle concentration in the flow. The flow Reynolds number has been observed to be directly linked with turbulence levels and, more interestingly, due to changes in boundary layer thickness, the turbulence profile along the flow cross section is different.

Finally, the phenomena associated with surface deformation, has proved to be the main flow characteristic that influences the velocity profile, turbulence energy production and shear stresses.

ACKNOWLEDGEMENTS

The authors express their gratitude to the CLIMEROD project financed through the EU contract MAS3-CT98-0166.

REFERENCES

Azzopardi, B.J. and Teixeira, J.C.F. (1994). "Detailed measurements of vertical annular two phase flow, part II: Gas core turbulence". ASME Journal of Fluids Engineering, 116(4).

Costa, M.A.V, Teixeira, S.F.C.F. and Teixeira, J.C.F. (2001). "Contribution to the turbulence of entrained particles in suspension", CLIMEROD interim report A8.

Graham, D.I., James, P.W., Jones, T.E.R., Davies, J.M. and Delo, E.A. (1992). "Measurement and prediction of surface shear stress in annular flume", Journal of Hydraulic Engineering, 118(9), pp. 1270-1286.

Hetsroni, G. (1989). "Particles-turbulence interaction", Int. Journal Multiphase Flow, 15(5), pp. 735-746.

Kleinhans, M.G. (2001). "The key role of fluvial dunes in transport and deposition of sand-gravel mixtures, a preliminary note", Sedimentary Geology, 143, pp 7-13.

Krogstad, P.A. and Antonia, R.A. (1999). "Surface roughness effects in turbulent boundary layers". Experiments in Fluids, 27, pp. 450-460.

Prent, M.T.H. and Hickin, E.J. (2001). "Annual regime of bedforms, roughness an flow resistance, Lillooet River, British Columbia, BC", Geomorphology, 41, pp. 369-390.

Soulsby, R. (1997). "Dynamics of Marine Sands", Thomas Telford: London, pp. 131-157.